The glassy random laser: replica symmetry breaking in the intensity fluctuations of emission spectra

F. Antenucci[1,2], **A. Crisanti**[2,3] **and L. Leuzzi**[1,2*]

[1] *NANOTEC-CNR, Institute of Nanotechnology, Soft and Living Matter Laboratory, Rome, Piazzale A. Moro 2, I-00185, Roma, Italy*

[2] *Dipartimento di Fisica, Università di Roma "Sapienza", Piazzale A. Moro 2, I-00185, Roma, Italy*

[3] *ISC-CNR, UOS Sapienza, Piazzale A. Moro 2, I-00185, Roma, Italy*

(Dated: June 12, 2015)

The behavior of a newly introduced overlap parameter is analyzed, measuring the correlation between intensity fluctuations of waves in random media in different physical regimes, with varying amount of disorder and non-linearity. Its relationship is established to the standard Parisi overlap order parameter in replica theory for spin-glasses. In the complex spherical spin-glass model, describing the onset and behavior of random lasers, replica symmetry breaking in the intensity fluctuation overlap is shown to occur at high pumping or low temperature. This order parameter identifies the laser transition in random media and describes its glassy nature in terms of emission spectra data, the only data so far accessible in random laser measurements. The theoretical analysis is, eventually, compared to recent intensity fluctuation overlap measurements demonstrating the validity of the theory and providing a straightforward interpretation of different spectral behaviors in different random lasers.

arXiv:1412.8748v3 [cond-mat.stat-mech] 11 Jun 2015

Introduction

Light amplification and propagation through random media have attracted much attention in recent years, with present-day applications to, e.g., speckle-free imaging and biomedical diagnostics [1], chip-based spectrometers [2–4], laser paints [5] and cryptography [6]. Whatever the amplifying medium, ordered or random, in a closed or in an open cavity, two are the basic ingredients to produce laser in any optically active system: *amplification* and *feedback*. In closed cavities the electromagnetic modes straightforwardly depend on the cavity geometry. In cavity-less random media, instead, some kind of modes are established by spontaneous emission and are localized in closed photonic trajectories by means of multiple scattering. Indeed, the phenomenon of *amplified spontaneous emission* (ASE) can occur even in systems without any optical cavity, whose fluorescence spectrum is simply determined by the gain curve of the active medium [7–12]. When, because of an external pumping, the multiple-scattering feedback process becomes strong, amplification by *stimulated* emission is established in the random medium and we have a *Random Laser* (RL) [13]. The feedback is, here, associated to the existence of well-defined long-lived localized modes, characterized by a definite frequency and a spatial pattern of the electromagnetic field inside the material. Modes are expressed as *slow amplitude* contributions to the electromagnetic field expansion in terms of spatial mode eigenvectors $\boldsymbol{E}_k(\boldsymbol{r})$:

$$\boldsymbol{E}(\boldsymbol{r},t) = \sum_k a_k(t)\ \boldsymbol{E}_k(\boldsymbol{r})\ e^{\imath\omega_k t} + \text{c.c.} \qquad (1)$$

The complex amplitudes $a_k(t)$ of these slow modes turn out to be the fundamental degree of freedom in the statistical mechanical modeling of interacting modes [14, 15], while the irregularity of their spatial profiles results into *quenched* disordered mode interactions. By quenched we mean that the interaction strengths are time independent [16], as it occurs, in practice, when they change on time-scales much longer then the typical amplification time-scales, possibly longer than the RL lifetime itself.

At least in some random media, the RL action presents the peculiar property of displaying strong non-trivial spectral fluctuations [17–22], i.e., narrow emission resonances appear to change frequency from one excitation pulse of the pumping laser to another one [23–26]. These will be termed *shot-to-shot* fluctuations from now on. If in spectral fluctuation measurements the scattering particles and all external experimental conditions are kept constant, these fluctuations will only be due to the initial configuration of pre-pumping electromagnetic modes occurring because of spontaneous emissions.

A connection to statistical mechanical models with quenched disordered interaction, i.e., spin-glass models [16, 27–29], has been recently established [14, 15, 30–33], providing a new point of view on the shot-to-shot fluctuations phenomenon. The leading mechanism for the non-deterministic activation of the modes is here identified with the frustration of the disordered interactions and the consequent presence of a large number of equivalent *states*. For *state* we mean a given ensemble of activated mode configurations, specified by their own wavelengths, phases and intensities, realized by very many emissions on time-scales of the order of the duration of the shot, that is, of the RL life-time itself. The diverse spectral realizations are, thus, conjectured to correspond to a glassy behavior consisting in many equivalent degenerate states constituting the RL regime. This glassy light regime is associated to an effective thermodynamic phase where the tendency of the modes to oscillate coherently in intensity is frustrated: in the language of the replica theory [27], it corresponds to a phase where the symmetry among equivalent replicas is spontaneously broken [34] and the

overlap (i.e., the similarity) between the configurations of the mode amplitudes display a nontrivial structure [15, 35]. Identical copies of the system show different amplitude equilibrium configurations, as the ergodicity is broken in many distinct states [36].

From an experimental point of view, the direct evaluation of the overlap between complex amplitudes and its probability distribution, i.e., the standard order parameter of the theory, requires the measure of the mode phases in the coherent regime. Such measure is not available so far, because of the low intensity of the RL emission (with respect to standard cavity lasers). The lack of a direct experimental knowledge of the whole overlap probability distribution is common, as well, to the original prototype systems for which replica symmetry breaking (RSB) theory was first developed, i.e., spin-glasses [37, 38], and also to structural glasses, one of the fields of major application of the theory [39–43].

An experimental validation of such *random-glassy* laser connection, and, particularly, of the RSB predicted by the theory, has, nevertheless, recently been put forward in Ref. [44], measuring the overlap between *intensity fluctuations* of the spectral emission. In the present work, we adopt a general model for cavity-less random lasers, in which not only the mode phases [30–33] but the whole complex amplitudes are considered as the fundamental degrees of freedom of the problem [14, 15]. In this framework we are able to demonstrate that RSB occurring in the standard amplitude overlap can, in principle, be observed in the intensity fluctuation overlap (actually a coarse-graining of the former) and viceversa. This development provides a theoretical setting to explain existing experimental results and to motivate similar measurements in diverse RL systems. Our approach also clarifies why RSB is found only in RL's in which mode couplings can be considered fixed (termed *quenched*) for all shots. In liquid compounds, instead, as a TiO_2 dispersion in Rhodamine B-ethylene glycol solution, no evidence for RSB is found [44].

The Complex Amplitude Model

The statistical approach we adopt is based on the hypothesis of effective equilibrium. The steady-state of a laser can be described as if at equilibrium at an effective temperature linked to the pumping rate of the source and to the true environment temperature (associated, e.g., to the noise of the spontaneous emission). In the mean-field limit, the photonic system is described in this framework by the general Hamiltonian [14, 15]

$$\mathcal{H} = -\frac{1}{2}\sum_{jk}^{1,N} J_{jk} a_j a_k^* - \frac{1}{4!}\sum_{jklm}^{1,N} J_{jklm} a_j a_k^* a_l a_m^* \,, \qquad (2)$$

where the sums are unrestricted and a_i are N complex amplitude variables subject to the global power constraint $\mathcal{E} = \epsilon N = \sum_k |a_k|^2$. The coupling strengths are here quenched independent random variables with mean $J_0^{(2)}/N^{p-1}$ and variance $p!\ J_p^2/(2N^{p-1})$ $(p = 2, 4)$, whose scaling with N guarantee an extensive Hamiltonian and thermodynamic convergence. For large N, the corresponding probability distribution can be taken Gaussian without loss of generality. Let us also define the degree of disorder $R_J = J_0/J$ and the pumping rate $\mathcal{P} = \epsilon\sqrt{\beta J_0}$ with $J_0 = J_0^{(2)} + J_0^{(4)}$ and $J = J_2 + J_4$, and where β is the inverse of the environment temperature.

This model can be derived in a multimode laser theory for open and irregular random resonators [15]. The openness of the cavity can be encoded into the definition of the electromagnetic modes using, e.g., the system-and-bath approach of Ref. [45], in which the contributions of radiative and localized modes are separated by Feshbach projection [46] onto two orthogonal subspaces. This leads to an effective theory on the subspace of localized modes in which they exchange a linear off-diagonal effective damping coupling [45, 47, 48]. In terms of the interaction parameters, we also define the strength of the openness as the inverse strength of the nonlinear interaction coupling with respect to the off-diagonal linear coupling $\alpha = J_4/J = J_0^{(4)}/J_0 \in [0, 1]$. In a closed cavity the linear dumping is absent and it corresponds to $\alpha = 1$.

In a standard semiclassical approach, the field is expressed in the slow amplitude basis, equation (1), where each mode displays a determined frequency. The lifetimes of these modes are assumed to be much longer than the characteristic times of population inversion and amplification processes, so that the atomic variables can be adiabatically removed and result in an effective interaction between the electromagnetic modes. The nonlinear couplings are, indeed, nonzero only for the terms $a_j a_k^* a_l a_m^*$ that meet the *frequency matching condition* [49–51],

$$|\omega_j - \omega_k + \omega_l - \omega_m| \lesssim \gamma \,, \qquad (3)$$

γ being the finite linewidth of the modes.

The mean-field approximation of the model equation (2) is exact when the probability distribution of the couplings is the same for all the mode couples (j, k) and tetrads (j, k, l, m). This is true, e.g., when mode localizations scale with the volume occupied by the active medium and their spectrum has a narrow-bandwidth around some given central frequency ω_0, i.e., $|\omega_j - \omega_0| < \gamma$, $\forall\ j$, so that the frequency matching condition, cf. equation (3), always holds.

Results

The Random Laser Transition. Given the quenched randomness of the J's, any observable depends on the particular realization of the disorder. Thus, the relevant quantity is the disorder averaged free energy $F = -\overline{\ln Z_J}/\beta$, where the overline denotes the average over the distribution of quenched disordered couplings. This can be analytically evaluated using the replica method [27, 37], as reported in the Methods. In this procedure the evaluation of the

relevant thermodynamic quantities is achieved considering n identical replicas (i.e., copies) of the system that act as probes exploring the multi-state phase space of the system. Further on, evaluating the distance between the replicas in terms of their similarity, termed *overlap*, one can retrieve the physical overlaps of the thermodynamic states [35].

In the complex amplitude spherical model, equation (2), the order parameter of the replica theory turns out to be given by the overlap between amplitudes of replica a and replica b:

$$Q_{\mathsf{ab}} = \frac{1}{N\epsilon}\sum_{k=1}^{N} a_k^{\mathsf{a}} \left(a_k^{\mathsf{b}}\right)^* \tag{4}$$

This Parisi overlap Q identifies the onset of a RL regime at a given critical value of the pumping, or, otherwise, at a critical temperature at fixed pumping, since random lasing is known to occur also decreasing temperature, besides increasing pumping [52–54]. Any nontrivial structure of the values taken by Q_{ab} implies that identical copies of the system, with the same interaction network and submitted to the same thermodynamic conditions, show different sets of values for microscopic observables at equilibrium and the ergodicity is broken in distinct equivalent states.

To our knowledge, from an experimental point of view, no phase correlation measurements, required for the evaluation of the complex amplitudes a_k^{a} and, consequently, of Q_{ab}, is available so far in random media. Only magnitudes $|a_k|$ are measured and not their phases $\phi_k = \arg(a_k)$. The experimental reconstruction of the distribution of the values of equation (4) is, thus, unfeasible.

Real Replicas. In recent experiments [44], shot-to-shot fluctuations of intensity spectra in an amorphous solid RL, a functionalized thiophene-based oligomer named thienyl-S,S-dioxide quinquethiophene (T5COx), are measured and analyzed. Since the sample remains under identical experimental conditions shot after shot, n different shots of RL emission correspond to n *real replicas* and one can measure the overlap between *intensity fluctuations* of two real replicas. In these experiments, the set of the activated modes emitting after the shot $\mathsf{a} = 1, \ldots, n$, whose available coarse-grained degree of freedom is the intensity $I_{\mathsf{a}}(k) = |a_k^{\mathsf{a}}|^2$, is observed to change from shot to shot.

When, during a single shot of the pumping source, the number of stimulated emission processes taking place is very large, the configurations of the mode dynamics can be considered as pertaining to a thermodynamic state. In terms of the *photonic bomb* language of Letohkov [10], e.g., this is a situation in which the typical amplification time is much shorter than the photons lifetime inside the medium, i.e., of the lifetime of stochastic resonators supporting the localized optical modes. The possible observation of numerous different states from shot to shot is, consequently, an evidence of a thermodynamic phase described by a corrugated free energy landscape composed of many valleys separated by barriers.

Intensity Fluctuation Overlap (IFO). Having as only experimentally available degree of freedom the intensities, one defines a suitable overlap based on their acquisition in different shots. To this aim, one first determines the average emission spectrum $\bar{I}(k) \equiv 1/n \sum_{\mathsf{a}=1}^{n} I_{\mathsf{a}}(k)$. Then, terming $\Delta_{\mathsf{a}}(k) \equiv I_{\mathsf{a}}(k) - \bar{I}(k)$ the intensity fluctuation of shot a around the average profile, one can define the overlap between the normalized intensity fluctuation of shots a and b as [44]:

$$\mathcal{C}_{\mathsf{ab}}^{\exp} \equiv \frac{\sum_k \Delta_{\mathsf{a}}(k)\Delta_{\mathsf{b}}(k)}{\sqrt{\sum_k \Delta_{\mathsf{a}}^2(k)}\sqrt{\sum_k \Delta_{\mathsf{b}}^2(k)}}, \tag{5}$$

where the index k denotes now the frequency, i.e., the experimental accessible equivalent of a mode index, depending on the spectral resolution. The overlap is measured between the fluctuations of intensity, rather than the straight intensities, to exclude the effects due to the amplified spontaneous emission. From n measured spectra one can calculate the $n(n-1)/2$ values of the IFO $\mathcal{C}_{\mathsf{ab}}^{\exp}$ and its distribution $P_J(\mathcal{C}^{\exp})$. Its average $P(\mathcal{C}^{\exp}) = \overline{P_J(\mathcal{C}^{\exp})}$ can be computed by repeated spectral measurements acquired on different samples. By different samples we, actually, mean different realizations of the microscopic disordered realization of scatterers positions as faced by the incoming pumping light beam. More precisely, one can realize a different realization by turning the material sample or, if the beam section is smaller than the random medium, by illuminating a different region with the pump laser spot.

If the variations of the normalization factors $\sqrt{\sum_k \Delta_{\mathsf{a}}^2(k)}$ in Eq. (5) are neglected with respect to fluctuations $\Delta_{\mathsf{a}}(k)$, in the $2+4$ complex amplitude model given by equation (2), the matrix

$$\mathcal{C}_{\mathsf{ab}} \equiv \frac{1}{8N\epsilon^2}\sum_{k=1}^{N}\left[\langle |a_k^{\mathsf{a}}|^2 |a_k^{\mathsf{b}}|^2\rangle - \langle |a_k^{\mathsf{a}}|^2\rangle\langle |a_k^{\mathsf{b}}|^2\rangle\right], \tag{6}$$

is the model equivalent of the IFO, up to an overall sign. Indeed, equation (6), defined in the dominion $[0, 1]$, holds with the prescription that $P(C_{\mathsf{ab}}^{\exp} = \mathcal{C})$ corresponds to $P(\mathcal{C}_{\mathsf{ab}} = |\mathcal{C}|)$. To compare with experimental results we will use symmetrized $P(\mathcal{C})$, $\mathcal{C} \in [-1:1]$, without any loss of generality.

IFO vs. standard overlap relationship. The average in equation (6) can be carried out using the replicated action derived in the Methods, cf. equation (13). This leads to the following relationship between the IFO and the standard order parameters:

$$\mathcal{C}_{\mathsf{ab}} = Q_{\mathsf{ab}}^2 - \frac{m^4}{4}, \quad \mathsf{a} \neq \mathsf{b}; \tag{7}$$

where Q_{ab} is defined in equation (4), and

$$m \equiv m_{\mathsf{a}}^{\sigma} = \frac{\sqrt{2}}{N} \sum_{k=1}^{N} \mathrm{Re}\,[a_k^{\mathsf{a}}]$$

is the parameter of global coherence (cf. Methods). According to equation (7), if a RSB occurs in the standard overlap Q_{ab} it propagates with the same structure to the IFO $\mathcal{C}_{\mathsf{ab}}$. We, thus, have a theoretical well funded tool to detect RSB in experimental data. We stress that this analysis could have not been possible in XY models with quenched amplitudes considered in previous works [30–32] because there the intensities of the modes are kept fixed during the mode dynamics.

In equation (7) we have considered the most general case in which a high pumping regime can display both a global coherence ($m \neq 0$) and a multi-state non-trivial structure for the amplitude configurations ($Q_{\mathsf{ab}} \neq 0$). This mixing physically occurs for a degree of disorder R_J next to the tolerance value beyond which standard mode locking (SML) breaks down, leaving place to random lasing. This is displayed in the phase diagrams in the central panels of the triptych figures 1 and 2, as the boundary lines between SML ($m \neq 0$) and purely random laser ($m = 0$ but $Q_{\mathsf{ab}} \neq 0$) at large $\mathcal{P}$.

The low pumping regime is replica symmetric for any R_J, with $m = 0$ and $Q_{\mathsf{ab}} = 0$ for $\mathsf{a} \neq \mathsf{b}$ [14], implying a Dirac delta probability $P(\mathcal{C})$, peaked in zero, both in the incoherent wave (IW) and in the phase locking wave (PLW) in figures 1 and 2 (cf. also Methods).

Replica Symmetric standard mode-locking laser. For no or weak disorder at high pumping $\mathcal{P}$, i.e., for a standard mode-locking laser in an ordered cavity [49, 50], for every $\mathsf{a} \neq \mathsf{b}$ the relationship $Q_{\mathsf{ab}} = \pm m^2/2$, with $m \neq 0$, holds between the overlap and the (replica independent) global coherence parameter. In other words, the ordered laser regime is replica symmetric, as well, and the $P(\mathcal{C})$ is a Dirac delta function in zero, once again. Remarkably, then, though in terms of the parameter m the standard mode locked regime is clearly different from the fluorescence regime, and so is $P(Q)$, cf. left panels $a - d$ of figures (1,2) and Refs. [14, 15], *the IFO distribution does not change below and above the standard mode-locking transition*. This has been observed in preliminary measurements on a Q-switched pulsed Nd-Yag standard laser in Ref. [44]. Indeed, the overlap of the model in equation (6) is between local fluctuations of intensity on different replicas, so a global ordering is invariably taken away (cf. Methods).

Onset of RSB across the random laser transition. For strong disorder, when the pumping increases above threshold, $\mathcal{P} > \mathcal{P}_c$, the replica symmetry is broken and the distribution of $\mathcal{C}_{\mathsf{ab}}$ becomes nontrivial, cf. panels *f, g, h* in figures 1 and 2.

Phase Diagrams and Overlap Distributions. Several scenarios are possible at the lasing transitions, exemplified in the paradigmatic cases of figures 1 and 2. In figure 1 we show the phase diagram and the behavior of the Parisi overlap distribution $P(Q)$ and its relative symmetrized IFO distribution $P(\mathcal{C})$ in a closed cavity ($\alpha = 1$) where linear dumping is absent. In figure 2 the behavior of $P(Q)$ and $P(\mathcal{C})$ is shown across the laser threshold in an open cavity ($\alpha = 0.4 < 1$), where the linear dumping is competing with non-linearity. In both the closed and the open cavity scenarios we illustrate two different critical regimes: the onset of standard mode locking at low disorder and the transition to random lasing for large R_J.

In a closed cavity situation, $\alpha = 1$, $P(Q)$ is discontinuous at the standard mode-locking laser transition, while $P(\mathcal{C})$ is unaffected. In this case the transition itself is discontinuous in the thermodynamic sense: the internal energy [14, 50] and the coherence parameter m (or the overlap $Q = \pm m^2/2$) are discontinuous, see left panel of the closed cavity triptych in figure 1. Here the distribution $P(Q)$ has two values trivially linked to the two possible values of the nonzero parameter, $m = \pm|m|$. At the RL transition ($R_J = 0.07$), alternatively, the $P(Q)$, and similarly $P(\mathcal{C})$, changes in a nontrivial way: two different values, a zero and a nonzero one, are possible as the pumping is increased. In this situation the RL regime is one step RSB (1RSB) and the transition is a so-called *random* first order (RFOT) in glassy physics terming [16] [55]: there is no latent heat [15], yet a new value for the overlap discontinuously appears at the transition, cf. right panel of figure 1.

In the cavity-less scenario $\alpha = 0.4$, instead, $P(Q)$ is continuous at the ordered ML transition. Indeed, a nonzero value for m increases continuously from zero as it can be observed looking at the peaks of $P(Q)$ in panels a and b of figure 2, where $Q = \pm m^2/2$. As in the closed cavity scenario, the $P(\mathcal{C})$ of the ordered ML laser does not change across the threshold. At the onset of the RL regime, illustrated for $R_J = 1.1$, the $P(\mathcal{C})$ is, instead, rather meaningful. At and just above the threshold, $P(\mathcal{C})$ displays a continuous part between the central peak in $\mathcal{C} = 0$ and the two side peaks, as displayed in panel h of figure 2. Here, the transition is thermodynamically continuous with a RL regime that is of the so-called full replica symmetry breaking (FRSB) kind, associated with a free energy landscape composed by a fractal hierarchy of valleys. As the pumping increases, the regime becomes 1+FRSB, a combination of 1RSB and FRSB solutions, with both a continuous and a discontinuous contribution to the probability distribution, cf. panel g in figure 2. The continuous parts in the $P(Q)$ and $P(\mathcal{C})$ depend on the influence of the off-diagonal damping term in J_{ij} in equation (2). For high enough pumping, well-above the threshold, the non-linear term eventually becomes dominant [15] and the solution, cf. panel h in figure 2, eventually becomes 1RSB, as in the closed cavity case, cf. panels *f, g, h* of figure 1.

In the RL experiment of Ref. [44] the distribution

$P(\mathcal{C}^{\rm exp})$, with $\mathcal{C}^{\rm exp}$ defined in equation (5) is peaked in zero at low pumping, while it becomes nontrivial with a triple and, eventually, double peaked shape as the lasing threshold is overcome. Although in comparison with the theoretical predictions for $N \to \infty$ the peaks of $P(\mathcal{C}^{\rm exp})$ are smeared by noise effects and finite modes' number effects, in all regimes $P(\mathcal{C}^{\rm exp}) \simeq P(-\mathcal{C}^{\rm exp})$. In figure 3 we display a comparison between the analytic IFO distribution computed in our $2+4$ complex amplitude spin-glass model, cf. equation (2), in an open cavity and the experimental measurements of $\mathcal{C}^{\rm exp}$ in Ref. [44, 56].

Discussion

In this work we provide the theoretical analytical background for a recently introduced order parameter [44] that allows to probe the phenomenon known as replica symmetry breaking in random lasers by means of experimentally accessible observables. These are shot-to-shot intensity fluctuations and the order parameter is the distribution of the values of the overlap between intensity fluctuations in different shots, as analytically defined in equation (6). Replica symmetry breaking is a known property occurring in mean-field glasses, spin-glasses and hard optimization problems. The parameters of the theory have never been measured, though, in any real system in these fields. In, particular, no measurement of the Parisi overlap and its distribution has been provided. The only experimental measure, so far, of a quantity possibly related to the standard RSB overlap been recently carried out on a photonic system. The system is an amplifying and scattering random medium, the T5COx, [44] displaying random lasing at high pumping. The parameter is the distribution of the shot-to-shot intensity fluctuations overlap (IFO). In the framework of a recently introduced general statistical mechanics theory of random photonic systems [14], in equation (20) we give here an analytic proof of the relationship between the IFO and the standard Parisi overlap, equation (4), and we provide measurable predictions for its behavior in both ordered and random lasing systems below and above threshold and, furthermore, both in the cases of discontinuous and continuous transitions to the laser regime at the threshold. In particular, the transition in the probability IFO distribution of a random laser is shown to be discontinuous (cf. figure 1) for closed (or controllable, limited open) cavities while it becomes continuous (cf. figure 2) for highly open cavity nonlinear wave systems. In the cavity-less case, where experimental measurements are available in at least one case, in figure 3 we compare theoretical and experimental behavior of the distributions of the IFO $\mathcal{C}$ from low to high pumping.

According to our results, a RSB is to be expected in random lasers whose random configurations of scatterers are fixed, i.e. *quenched*, for all analyzed shots. That is, the dynamics of their positions evolves on time-scales much longer than the whole experiment and real replicas can be realized. This is the experimental case of the solid/powder samples of random lasers as GaAs powders [54, 57], core-shell colloidal CdSe/ZnS quantum dots [58], ZnO powders [59] or pressurized pellets [60], and polymeric substances [44, 61, 62]. A notable counterexample might be porous gallium phosphide (GaP) filled with a solution of Rhodamine and methanol [63, 64], in which spectral fluctuations are reported to be minimal and the structure of the resonances, though random, appears to be reproducible from shot to shot. IFO measurements might yield, in this case, an ordered-like $P(\mathcal{C})$, peaked in zero both below and above threshold.

On the contrary, experiments on optically active random media whose scatterer particles sensitively move between subsequent shots in a single experiment, as in liquid solutions of Rhodamine and methanol with particles of Titanium oxide [65], Zinc oxide [66], pure Titania [67], or colloidal CdSe quantum dots [68] could establish no real replicas. Not having the same quenched disorder in all shots might prevent the observation of RSB. The overlap between copies of systems with different realizations of the disordered couplings, indeed, is known to be replica symmetric, as it has been shown in models with continuous spherical variables [69], of which our model in equation (2) is a generalization. Similarly to what happens in the ordered ML case, cf. left panels of figures 1 and 2, in that case the occurrence of a trivial single peaked $P(\mathcal{C})$ in $\mathcal{C}=0$ is expected, both below and above $\mathcal{P}_c$. Such a behavior has been observed in a liquid system of TiO_2 scattering nano-particle suspensions in solution of Rhodamine and methanol [44].

Eventually, we would like to stress that, besides a rigorous interpretation of recent experimental results for random lasers in terms of replica theory, our results provide an exciting and easily available test of spin-glass theory properties in continuous systems without local magnitude constraints, as disordered photonic systems.

Methods

Replica Theory and Order Parameters. The most complicated system that we are considering in our theory is a random system with disordered mode couplings that possibly display a high pumping/low temperature phase with ergodicity breaking and the occurrence of very many states. By "very many" we mean that their number scales with the size of the system, i.e. the number N of optically active modes. These states are not related by any simple relationship among them. That is, e.g., no simple Z_2 spin reversal symmetry occurs between states, as in the Ising model, nor $SU(2)$ symmetry as in the XY model. In the complex glassy case, to probe the multi-state disordered thermodynamic phase, one, thus, considers n copies of the system with exactly the same set of disordered couplings, the J's, and evaluates the disorder averaged partition function $\overline{Z_J^n}$ of the replicated system. A continuation to

real n is, then, taken to evaluate

$$-\beta F = \overline{\ln Z_J} = \lim_{n\to 0} \frac{\overline{Z_J^n} - 1}{n} \tag{8}$$

As a result, F is expressed as a functional in the replica space of the overlap matrices

$$Q_{\mathsf{ab}} = \frac{1}{N\epsilon} \sum_{k=1}^{N} \mathrm{Re}\big[a_k^{\mathsf{a}} \left(a_k^{\mathsf{b}}\right)^*\big], \tag{9}$$

$$R_{\mathsf{ab}} = \frac{1}{N\epsilon} \sum_{k=1}^{N} \mathrm{Re}\big[a_k^{\mathsf{a}}\, a_k^{\mathsf{b}}\big], \tag{10}$$

$\mathsf{a}, \mathsf{b} = 1, \ldots, n$ being replica indexes. The diagonal parts are

$$Q_{\mathsf{aa}} = \frac{1}{N\epsilon} \sum_{k=1}^{N} |a_k^{\mathsf{a}}|^2 = 1\,,$$

by definition of the total power constraint, and

$$R \equiv R_{\mathsf{aa}} = \frac{1}{N\epsilon} \sum_{k=1}^{N} |a_k^{\mathsf{a}}|^2\, e^{2\imath\phi_k}\,, \tag{11}$$

yielding information about global phase coherence. This parameter discriminates between the IW ($R = 0$) and the PLW ($R > 0$) regimes (cf. figures 1 and 2), in which all the other parameters are identical [14]

Alternatively, writing $a_k = \sqrt{\epsilon}\,(\sigma_k + \mathrm{i}\tau_k)$, we can define the overlaps of the real parts σ or the imaginary parts τ of the complex amplitudes:

$$A_{\mathsf{ab}} \equiv Q_{\mathsf{ab}} + R_{\mathsf{ab}} = \frac{2}{N} \sum_{k=1}^{N} \sigma_k^{\mathsf{a}} \sigma_k^{\mathsf{b}}\,,$$

$$B_{\mathsf{ab}} \equiv Q_{\mathsf{ab}} - R_{\mathsf{ab}} = \frac{2}{N} \sum_{k=1}^{N} \tau_k^{\mathsf{a}} \tau_k^{\mathsf{b}}\,. \tag{12}$$

As the system size becomes sufficiently large, the free energy sample-to-sample fluctuations die out and the free energy, equation (8), becomes independent of disorder, i.e., it is *self- averaging*. For $N \to \infty$ the physical value of the matrices follows from the extremization of the free energy functional. Because of the fact that the number of independent elements of an overlap matrix is $n(n-1)/2$ (taken away the diagonal) in the limit $n \to 0$ the usual minimization of the thermodynamic potential actually becomes a maximization in the space of the overlap matrices. To maximize F, a non-trivial Ansatz on the structure of Q and R is necessary. Indeed, it can be shown [14] that the most intuitive *replica symmetric* solution, with Q_{ab} and R_{ab} independent of a and b, does not lead to a thermodynamically stable solution in the whole phase space: beyond the critical point, in the glassy phase, one must, hence, resort to spontaneous RSB. Following the Parisi scheme [27] the overlap matrices are, then, taken $\mathcal{R}$-step RSB matrix, with $\mathcal{R} \to \infty$ for a continuous full RSB (FRSB). These are block matrices where the number of inner blocks $\mathcal{R}+1$ corresponds to the number of hierarchical levels in the multi-state phase space.

Depending on the value of $J_{2,4}$ the solution of the RL model Eq. (2) displays phases with different RSB structures, ranging from 1RSB, FRSB to a combination of discontinuous one step and continuous breaking (1+FRSB) [70].

Replicated Action. In the replica formalism, the averages of an observable $O[\{a\}]$ over the equilibrium Gibbs distribution and over the quenched disorder can be written as

$$\overline{\lim_{n\to 0} Z_J^{n-1} \int \prod_{k=1}^{N} da_k^* da_k\; O[\{a\}]\; e^{-\beta\mathcal{H}[\{a;J\}]}}$$
$$= \lim_{n\to 0} \int \prod_{a=1}^{n} da_{\mathsf{a}}^\star da_{\mathsf{a}}\; O[\{a\}]\; e^{\mathcal{S}[a]} \equiv \langle O[\{a\}]\rangle$$

where the average $\langle \ldots \rangle$ *in the replica space* is evaluated with the replicated action

$$\mathcal{S} = -\frac{1}{2} \sum_{\mathsf{a},\mathsf{b}=1}^{n} \sigma_{\mathsf{a}}\, (\mathcal{A})^{-1}_{\mathsf{ab}}\, \sigma_{\mathsf{b}} + \sum_{\mathsf{a}=1}^{n} h_{\mathsf{a}}^{\sigma}\, \sigma_{\mathsf{a}}$$
$$-\frac{1}{2} \sum_{\mathsf{a},\mathsf{b}=1}^{n} \tau_{\mathsf{a}}\, (\mathcal{B})^{-1}_{\mathsf{ab}}\, \tau_{\mathsf{b}} + \sum_{\mathsf{a}=1}^{n} h_{\mathsf{a}}^{\tau}\, \tau_{\mathsf{a}} \tag{13}$$

Here we have introduced the matrices

$$\mathcal{A} \equiv A - \vec{m}^{\sigma} \otimes \vec{m}^{\sigma}, \qquad \mathcal{B} \equiv B - \vec{m}^{\tau} \otimes \vec{m}^{\tau}. \tag{14}$$

and the effective fields

$$h^{\sigma,\tau} \equiv 2m^{\sigma,\tau} \left\{ b_2 + 2b_4 \left[(m^{\sigma})^2 + (m^{\tau})^2 \right] \right\} \tag{15}$$

These are functions of the *global coherence* parameters

$$m_{\mathsf{a}}^{\sigma} = \frac{\sqrt{2}}{N} \sum_{k=1}^{N} \sigma_k^{\mathsf{a}}\,, \qquad m_{\mathsf{a}}^{\tau} = \frac{\sqrt{2}}{N} \sum_{k=1}^{N} \tau_k^{\mathsf{a}}, \tag{16}$$

analogous to the magnetization for spin models, with coefficients $b_2 = \beta J_0^{(2)} \epsilon/4$, $b_4 = \beta J_0^{(4)} \epsilon^2/96$. After some algebra (see Ref. [15] for details), the field $h^{\sigma,\tau}$ can be expressed as

$$h^{\sigma} \equiv \frac{m^{\sigma}}{\sum_c A_{ac}}, \qquad h^{\tau} \equiv \frac{m^{\tau}}{\sum_c B_{ac}}. \tag{17}$$

For weak disorder (low R_J) the global coherence $m^{\sigma,\tau}$ is non-zero above the lasing threshold and must be included into the description. If disorder is strong, though, in the frozen glassy phase, the global coherence is null: $m^{\sigma,\tau} = 0$.

Because it turns out that $\langle \sigma_{\mathsf{a}} \tau_{\mathsf{b}} \rangle = 0$ [14, 15], the integrals in the σ, τ space factorize and the IFO $\mathcal{C}_{\mathsf{ab}}$ defined in equation (6) takes the form

$$\mathcal{C}_{\mathsf{ab}} = \frac{1}{8} \left(\langle \sigma_{\mathsf{a}}^2 \sigma_{\mathsf{b}}^2 \rangle + \langle \tau_{\mathsf{a}}^2 \tau_{\mathsf{b}}^2 \rangle - \langle \sigma^2 \rangle^2 - \langle \tau^2 \rangle^2 \right), \tag{18}$$

where $\langle\sigma^2\rangle = \langle\sigma_{\mathsf{a}}^2\rangle$ and $\langle\tau^2\rangle = \langle\tau_{\mathsf{a}}^2\rangle$, since single replica quantities do not depend on the replica index.

The replicated action $\mathcal{S}$ given in equation (13) is quadratic. Thus, using the Wick's theorem, for the averages in equation (18) we easily obtain

$$\mathcal{C}_{\mathsf{ab}} = \frac{\mathcal{A}_{\mathsf{ab}}^2}{4} + \frac{\mathcal{A}_{\mathsf{ab}}\,(m^\sigma)^2}{2} + \frac{\mathcal{B}_{\mathsf{ab}}^2}{4} + \frac{\mathcal{B}_{\mathsf{ab}}\,(m^\tau)^2}{2} \tag{19}$$

Equation (19) can be further simplified since the physical solutions of the model are either of the form $Q_{\mathsf{ab}} = R_{\mathsf{ab}}$ or $Q_{\mathsf{ab}} = -R_{\mathsf{ab}}$ ($\mathsf{a} \neq \mathsf{b}$). Since the two solutions are equivalent, without loss of generality we choose the first one, so that $m^\tau = 0$ and equation (19) leads to

$$\mathcal{C}_{\mathsf{ab}} = Q_{\mathsf{ab}}^2 - \frac{m^4}{4}\,, \quad \mathsf{a} \neq \mathsf{b}\,; \tag{20}$$

$$\mathcal{C}_{\mathsf{aa}} = \frac{1+R^2}{2} - \frac{m^4}{4} \tag{21}$$

where Q_{ab} is defined in equation (4),

$$R \equiv R_{\mathsf{aa}} = \frac{1}{\epsilon N}\sum_{k=1}^{N} \mathrm{Re}\left[(a_k^{\mathsf{a}})^2\right] \tag{22}$$

is the parameter of partial coherence, cf. equation (11), and

$$m \equiv m_{\mathsf{a}}^\sigma = \frac{\sqrt{2}}{N}\sum_{k=1}^{N} \mathrm{Re}\left[a_k^{\mathsf{a}}\right] \tag{23}$$

is the parameter of global coherence [14, 15]. Equation (20) is one of our main results and is discussed in the main text, cf. equation (7).

* luca.leuzzi@cnr.it

References.

[1] B. Redding, M. A. Choma, and H. Cao, "Speckle-free laser imaging using random laser illumination," Nature Photon. **6**, 497 (2012).

[2] B. Redding and H. Cao, "Using a multimode fiber as a high-resolution low-loss spectrometer." Opt. Lett. **37**, 3384 (2012).

[3] B. Redding, S. M. Popoff, and H. Cao, "All-fiber spectrometer based on speckle pattern reconstruction," Opt. Expr. **21**, 6584 (2013).

[4] B. Redding, S. F. Liew, R. Sarma, and H. Cao, "Compact spectrometer based on a disordered photonic chip," Nature Photon. **7**, 746 (2013).

[5] S. John and G. Pang, "Theory of lasing in a multiple-scattering medium," Phys. Rev. A **54**, 3642–3652 (1996).

[6] R. Horstmeyer, B. Judkewitz, I. M. Vellekoop, S. Assawaworrarit, and C. H. Yang, "Physical key-protected one-time pad," Sci. Rep. **3**, 3543 (2013).

[7] R. V. Ambartsumyan, N. G. Basov, P. G. Kryukov, and V. S. Lethokov, "A laser with nonresonant feedback," JETP **24**, 481 (1967).

[8] R. V. Ambartsumyan, P. G. Kryukov, and V. S. Lethokov, "Dynamics of emission line narrowing for a laser with nonresonant feedback," JETP **24**, 1129 (1967).

[9] R. V. Ambartsumyan, P. G. Kryukov, and Yu. A. Lethokov, V. S.and Matveets, "Statistical emission properties of a nonresonant feedback laser," JETP **26**, 1109 (1968).

[10] VS Letokhov, "Generation of light by a scattering medium with negative resonance absorption," Soviet JETP **26**, 835 (1968).

[11] V M Markushev, V F Zolin, and Ch M Briskina, "Luminescence and stimulated emission of neodymium in sodium lanthanum molybdate powders," Sov. J. Quantum Elec. **16**, 281 (1986).

[12] C Gouedard, D Husson, C Sauteret, F Auzel, and A Migus, "Generation of spatially incoherent short pulses in laser-pumped neodymium stoichiometric crystals and powders," JOSA B **10**, 2358–2363 (1993).

[13] Diederik S. Wiersma and Ad Lagendijk, "Light diffusion with gain and random lasers," Phys. Rev. E **54**, 4256–4265 (1996).

[14] F. Antenucci, C. Conti, A. Crisanti, and L. Leuzzi, "General phase diagram of multimodal ordered and disordered lasers in closed and open cavities," Phys. Rev. Lett. **114**, 043901 (2015).

[15] F. Antenucci, A. Crisanti, and L. Leuzzi, "The complex spherical spin 2+4 spin-glass model: applications to optics," Phys. Rev. A (2015).

[16] G. Parisi, "Spin glasses and fragile glasses: Statics, dynamics, and complexity," PNAS **103**, 7948 (2006).

[17] S. E. Skipetrov and R. Maynard, "Instabilities of waves in nonlinear disordered media," Phys. Rev. Lett. **85**, 736 (2000).

[18] D. Anglos, A. Stassinopoulos, R. N. Das, G. Zacharakis, M. Psyllaki, R. Jakubiak, R. A. Vaia, E. P. Giannelis, and S. H. Anastasiadis, "Random laser action in organic–inorganic nanocomposites," J. Opt. Soc. Am. B **21**, 208–213 (2004).

[19] K. L. van der Molen, A. P. Mosk, and A. Lagendijk, "Intrinsic intensity fluctuations in random lasers." Phys. Rev. A **74**, 053808 (2006).

[20] Stefano Lepri, Stefano Cavalieri, Gian-Luca Oppo, and Diederik S. Wiersma, "Statistical regimes of random laser fluctuations," Phys. Rev. A **75**, 063820 (2007).

[21] S. Mujumdar, V. Türeci, R. Torre, and D. S. Wiersma, "Chaotic behavior of a random laser with static disorder," Phys. Rev. A **76**, 033807 (2007).

[22] J. Fallert, R. J. B. Dietz, J. Sartor, D. Schneider, C. Klingshirn, and H. Kalt, "Co-existence of strongly and weakly localized random laser modes." Nat. Photon. **3**, 279282 (2009).

[23] H. Cao, Y. G. Zhao, H. C. Ong, S. T. Ho, J. Y. Dai, J. Y. Wu, and R. P. H. Chang, "Ultraviolet lasing in resonators formed by scattering in semiconductor polycrystalline films," Appl. Phys. Lett. **73**, 3656–3658 (1998).

[24] Y. Ling, H. Cao, A. L. Burin, M. A. Ratner, X. Liu, and R. P. H. Chang, "Investigation of random lasers with resonant feedback," Phys. Rev. A **64**, 063808 (2001).

[25] H. Cao, Y. Ling, J. Y. Xu, C. Q. Cao, and Prem Kumar, "Photon statistics of random lasers with resonant feedback," Phys. Rev. Lett. **86**, 4524–4527 (2001).

[26] T. Nakamura, H. Fujiwara, R. Niyuki, K. Sasaki, Y. Ishikawa, N. Koshizaki, T. Tsuji, and S. Adachi, "Origins of lasing emission in a resonance-controlled zno

random laser," New J. Phys. **16**, 093054 (2014).
[27] M. Mézard, G. Parisi, and M. A. Virasoro, *Spin glass theory and beyond* (World Scientific, Singapore, 1987).
[28] Francesco Guerra, "Spontaneous replica symmetry breaking in the mean field spin glass model," in *New Trends in Mathematical Physics* (Springer, Berlin (Germany), 2009) pp. 299–311.
[29] Michel Talagrand, *Mean Field Models for Spin Glasses* (Springer, Berlin, 2011).
[30] L. Angelani, C. Conti, G. Ruocco, and F. Zamponi, "Glassy behavior of light," Phys. Rev. Lett. **96**, 065702 (2006).
[31] L. Angelani, C. Conti, G. Ruocco, and F. Zamponi, "Glassy behavior of light in random lasers," Phys. Rev. B **74**, 104207 (2006).
[32] L. Leuzzi, C. Conti, V. Folli, L. Angelani, and G. Ruocco, "Phase diagram and complexity of mode-locked lasers: From order to disorder," Phys. Rev. Lett. **102**, 083901 (2009).
[33] C. Conti and L. Leuzzi, "Complexity of waves in nonlinear disordered media," Phys. Rev. B **83**, 134204 (2011).
[34] G. Parisi, "Infinite number of order parameters for spin-glasses," Phys. Rev. Lett. **43**, 1754–1756 (1979).
[35] G. Parisi, "Order parameter for spin-glasses," Phys. Rev. Lett. **50**, 1946–1948 (1983).
[36] G. Parisi, "Lack of ergodicity in the infinite-range ising spin-glass," Phys. Rev. Lett. **49**, 301–304 (1982).
[37] S. F. Edwards and P. W. Anderson, "Theory of spin glasses," J. Phys. F **5**, 965 (1975).
[38] David Sherrington and Scott Kirkpatrick, "Solvable model of a spin-glass," Phys. Rev. Lett. **35**, 1792–1796 (1975).
[39] M. Mézard and G. Parisi, "A first principle computation of the thermodynamics of glasses," J. Chem. Phys. **111**, 1076 (1999).
[40] G. Parisi and F. Zamponi, "Mean field theory of hard sphere glasses and jamming," Rev. Mod. Phys. **82**, 789 (2010).
[41] F. Caltagirone, U. Ferrari, L. Leuzzi, G. Parisi, F. Ricci-Tersenghi, and T. Rizzo, "Critical slowing down exponents of mode coupling theory," Phys. Rev. Lett. **108**, 085702 (2012).
[42] S. Franz, H. Jacquin, G. Parisi, P. Urbani, and F. Zamponi, "Quantitative field theory of the glass transition," PNAS **109**, 18725 (2012).
[43] P. Charbonneau, J. Kurchan, G. Parisi, P. Urbani, and F. Zamponi, "Fractal free energy landscapes in structural glasses," Nat. Commun. **5**, 3725 (2014).
[44] N. Ghofraniha, I. Viola, F. Di Maria, G. Barbarella, G. Gigli, L. Leuzzi, and C. Conti, "Experimental evidence of replica symmetry breaking in random lasers," Nat. Commun. **6**, 6058 (2015).
[45] C. Viviescas and G. Hackenbroich, "Field quantization for open optical cavities," Phys. Rev. A **67**, 013805 (2003).
[46] Herman Feshbach, "A unified theory of nuclear reactions. {II}," Ann. Phys. **19**, 287 – 313 (1962).
[47] G. Hackenbroich, C. Viviescas, and F. Haake, "Field quantization for chaotic resonators with overlapping modes," Phys. Rev. Lett. **89**, 083902 (2002).
[48] C. Viviescas and G. Hackenbroich, "Quantum theory of multimode fields: applications to optical resonators," J. Opt. B **6**, 211 (2004).
[49] H. A. Haus, "Mode-locking of lasers," IEEE J. Quantum Electron. **6**, 1173–1185 (2000).
[50] Ariel Gordon and Baruch Fischer, "Phase transition theory of many-mode ordering and pulse formation in lasers," Phys. Rev. Lett. **89**, 103901 (2002).
[51] F. Antenucci, M. Ibañez Berganza, and L. Leuzzi, "Statistical physical theory of mode-locking laser generation with a frequency comb," Phys. Rev. A **91**, 043811 (2015).
[52] D. S. Wiersma and S. Cavalieri, "Light emission: a temperature-tunable random laser," Nature **414** (2001).
[53] D. S. Wiersma and S. Cavalieri, "Light emission: a temperature-tunable random laser," Phys. Rev. E **66**, 056612 (2002).
[54] T. Nakamura, T. Takahashi, and S. Adachi, "Temperature dependence of gaas random laser characteristics," Phys. Rev. B **81**, 125324 (2010).
[55] In the RFOT scenario the static (ideal) glass transition is preceded by a glassy dynamic arrest (drawn as a dashed line in the central panel of figure 1) [14, 15]: a photonic system in this case should show the typical two-step dynamical relaxation for the time correlation function of light modes, in the same universality class of the mode-coupling theory for structural glasses.
[56] N. Ghofraniha, I. Viola, F. Di Maria, G. Barbarella, G. Gigli, L. Leuzzi, and C. Conti, "Corrigendum: Experimental evidence of replica symmetry breaking in random lasers," Nat. Commun. **6**, 6300 (2015).
[57] M. A. Noginov, G. Zhu, I. Fowlkes, and M. Bahoura, "Gaas random laser," Laser Phys. Lett. **1**, 291293 (2004).
[58] Y. Chen, J. Herrnsdorf, B. Guilhabert, Y. Zhang, I. M. Watson, E. Gu, N. Laurand, and M. D. Dawson, "Colloidal quantum dot random laser," Opt. Expr. **19**, 2996 (2011).
[59] H. Cao, Y. G. Zhao, S. T. Ho, E. W. Seelig, Q. H. Wang, and R. P. H. Chang, "Random laser action in semiconductor powder," Phys. Rev. Lett. **82**, 2278–2281 (1999).
[60] H. Cao, Y. Ling, J. Y. Xu, C. Q. Cao, and P. Kumar, "Photon statistics of random lasers with resonant feedback," Phys. Rev. Lett. **86**, 4524 (2001).
[61] Lee C. W., K. S. Wong, J. D. Huang, S. V. Frolov, and Z. V. Vardeny, "Femtosecond time-resolved laser action in polyphenylene vinylene films: stimulated emission in an inhomogeneously broadened exciton distribution," Chem. Phys. Lett. **314**, 564569 (1999).
[62] M. Anni, S. Lattante, T. Stomeo, R. Cingolani, G. Gigli, G. Barbarella, and L. Favaretto, "Modes interaction and light transport in bidimensional organic random lasers in the weak scattering limit," Phys. Rev. B **70**, 195216 (2004).
[63] K. L. van der Molen, R. W. Tjerkstra, A. P. Mosk, and A. Lagendijk, "Spatial extent of random laser modes," Phys. Rev. Lett. **98**, 143901 (2007).
[64] R. G. S. El-Dardiry, A.P. Mosk, O. L. Muskens, and A. Lagendijk, "Experimental studies on the mode structure of random lasers," Phys. Rev. A **81**, 043830 (2010).
[65] N. M. Lawandy, Balachandran R. M., A. S. L. Gomes, and E. Sauvain, "Laser action in strongly scattering media," Nature **368**, 436–438 (1994).
[66] H. Cao, J. Y. Xu, S.-H. Chang, and S. T. Ho, "Transition from amplified spontaneous emission to laser action in strongly scattering media," Phys. Rev. E **61**, 1985 (2000).
[67] R. G. S. El-Dardiry, R. Mooiweer, and A. Lagendijk, "Experimental phase diagram for random laser spectra," New J. Phys. **14**, 113031 (2012).
[68] A. K. Augustine, P. Radhakrishnan, V. P. N. Nampoori, and M. Kailasnath, "Enhanced random lasing from a colloidal cdse quantum dot-rh6g system," Laser Phys.

Lett. **12**, 025006 (2015).
[69] H.-W. Chen, W-K. andi Hsieh, C.-R. Hwang, and Y.-C. Sheu, "Disorder chaos in the spherical mean-field model," J. Stat. Phys. (2015).
[70] A. Crisanti and L. Leuzzi, "Exactly solvable spin glass models with ferromagnetic couplings: The spherical multi-p-spin model in a self-induced field," Nucl. Phys. B **870**, 176 (2013).

Acknowledgments. We thank Silvio Franz for stimulating this work and for interesting discussions. The research leading to these results has received funding from the People Programme (Marie Curie Actions) of the European Union's Seventh Framework Programme FP7/2007-2013/ under REA grant agreement n. 290038, NETADIS project, from the European Research Council through ERC grant agreement no. 247328 - CriPheRaSy project - and from the Italian MIUR under the Basic Research Investigation Fund FIRB2008 program, grant No. RBFR08M3P4, and under the PRIN2010 program, grant code 2010HXAW77-008.

Author contributions statement. F.A., A.C and L.L. conceived the theory, performed the computations and wrote the manuscript.

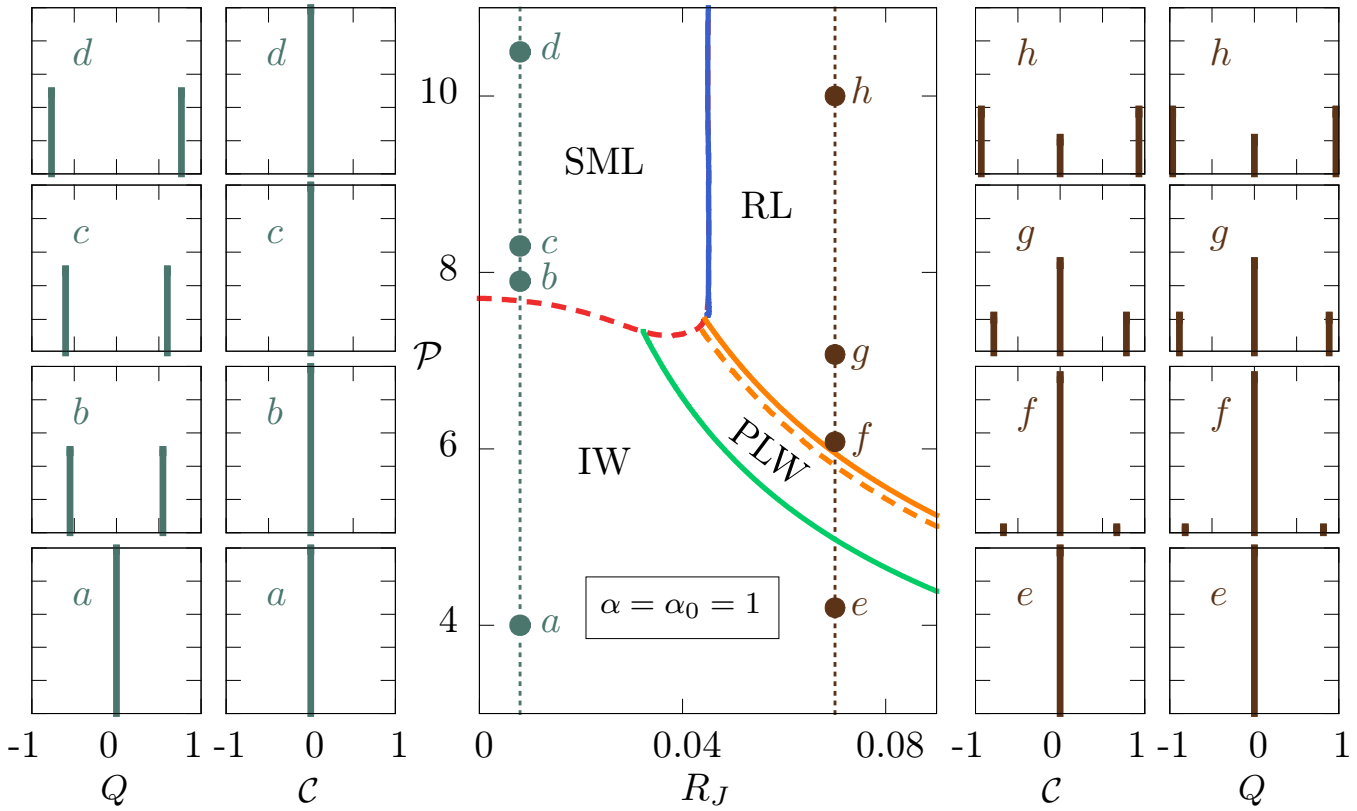

Figure 1. Laser transition triptych in a closed cavity for varying disorder. In the central panel the phase diagram $(\mathcal{P}, R_J)$ is displayed for a closed cavity (nonlinearity strength $\alpha = 1$) in terms of the four possible optical regimes [14, 15]: incoherent wave (IW), standard mode locking (SML), phase locking wave (PLW) and random laser (RL). Two pumping paths across the lasing tresholds are shown as dotted lines, at $R_J = 0.01$ $[\mathcal{P} = 4.00(a), 7.90(b), 8.30(c), 10.5(d)]$ and $R_J = 0.07$ $[\mathcal{P} = 4.20(e), 6.08(f), 7.07(g), 10.0(h)]$. In the left panels a to d the behavior the distributions of IFO, $P(\mathcal{C})$, and standard overlap, $P(Q)$, across the ordered ML laser threshold are reported. The transition is discontinuous in the standard Parisi distribution $P(Q)$, whereas $P(\mathcal{C})$ is invariant. In the right panels e to h the IFO and standard overlap distributions are shown for the RL transition: as $\mathcal{P}$ increases, we show that the low $\mathcal{P}$ solution is replica symmetric (e), while above threshold it becomes discontinuously 1RSB (f, g, h).

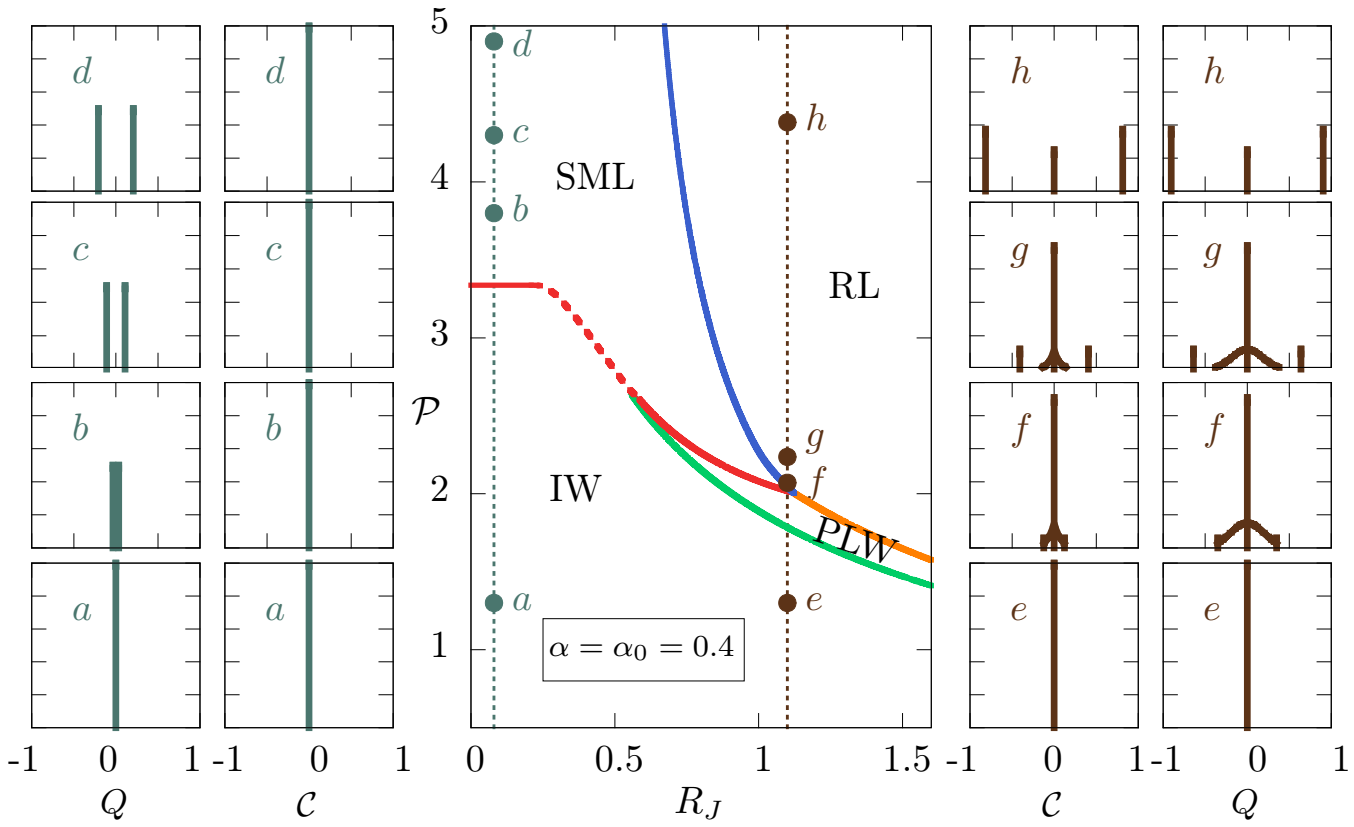

Figure 2. Laser transition triptych in an open cavity for varying disorder. In the central panel the phase diagram $(\mathcal{P}, R_J)$ is displayed for an open cavity (nonlinearity strength $\alpha = 0.4$) in terms of the four possible optical regimes [14, 15]: incoherent wave (IW), standard mode locking (SML), phase locking wave (PLW) and random laser (RL). Two pumping paths across the lasing tresholds are shown as dotted lines, at $R_J = 0.07$ [$\mathcal{P} = 1.30(a), 3.80(b), 4.30(c), 4.90(d)$] and $R_J = 1.1$ [$\mathcal{P} = 1.30(e), 2.05(f), 2.35(g), 4.38(h)$]. In the left panels a to d the behavior of IFO and standard overlap distributions across the ordered ML laser threshold are reported. The transition is now continuous in the order parameters $P(Q)$, while $P(\mathcal{C})$ does not change below and above threshold. In the right panels e to h the IFO and standard overlap distributions are shown for the RL transition. As $\mathcal{P}$ increases we show that the low optical power solution is replica symmetric (e), soon above threshold the solution is FRSB (f), further increasing $\mathcal{P}$ the solution becomes 1+FRSB (g) and, eventually, for large pumping it is 1RSB (h). The transition is continuous in the order parameters $P(Q, \mathcal{C})$.

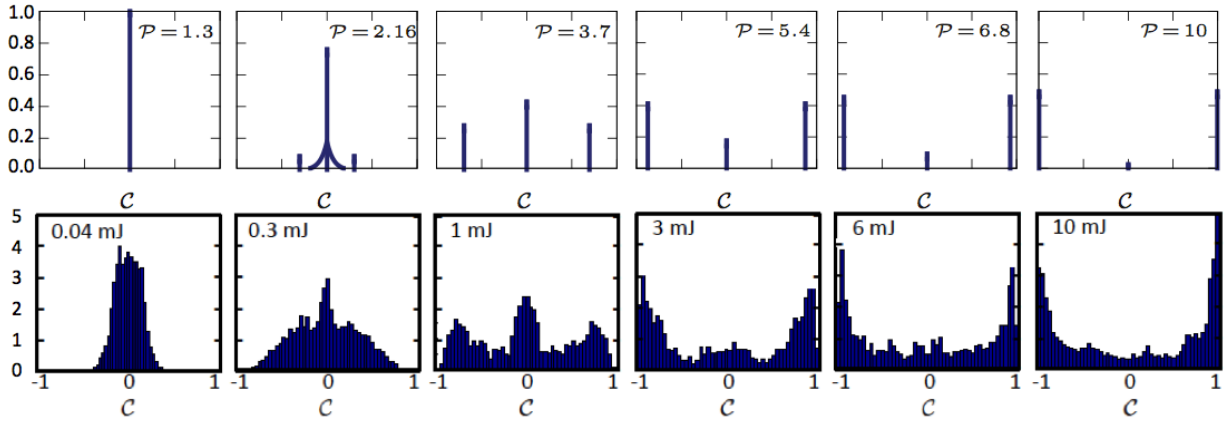

Figure 3. Comparison between theory and experiments in a cavity less random laser. In the top row we display the probability distributions of the IFO for $\alpha = 0.4$, when linear and nonlinear interactions are competing, $R_J = 1.1$ and for increasing pumping. Vertical lines represent Dirac's deltas, whose height is the probability of the argument value. Different regimes are represented from fluorescence to large pumping random lasing. They are chosen along the dotted line in figure 2 at $R_J = 1.1$. Form left to right the first distribution is at point e in figure 2, the second between f and g, the third one between g and h and the following above h. In the bottom row the same regimes are reproduced in the IFO distribution experimentally measured and reported in Ref. [44, 56] in an amorphous solid oligomeric random laser, T5COx.